

## SINGLE-TOP-QUARK PHYSICS AT THE TEVATRON\*

CATALIN I. CIOBANU

for the CDF and DØ Collaborations

LPNHE Univ. Paris VI and VII, IN2P3-CNRS  
4 Place Jussieu, 75252 Paris Cedex 05, France*(Received January 8, 2008)*

In this document we present the status of the searches for the electroweak production of top quarks (single-top-quarks) at the CDF and DØ experiments at the Tevatron.

PACS numbers: 14.65.Ha, 12.15.Hh, 12.15.Ji

**1. Introduction**

According to the Standard Model, in  $p\bar{p}$  collisions at the Tevatron top quarks can be created in pairs via the strong force, or singly via the electroweak interaction. The latter production mode is referred to as “single-top-quark” production and takes place mainly through the  $t$ - or  $s$ -channel exchange of a  $W$  boson. Studying single-top production at hadron colliders [1] is important for a number of reasons. First, it provides a window into measuring the Cabibbo–Kobayashi–Maskawa (CKM) matrix element  $|V_{tb}|^2$ , which in turn is closely tied to the number of quark generations. Second, measuring the spin polarization of single-top quarks can be used to test the  $V$ – $A$  structure of the top weak charged current interaction. Third, the estimation of the single-top backgrounds is crucial for several searches for other signals (*e.g.* Higgs boson). Fourth and last, the presence of various new SM and non-SM phenomena may be inferred by observing deviations from the predicted rate of the single-top signal.

The theoretical single-top production cross section is  $\sigma_{s+t} = 2.9$  pb for a top mass of  $175 \text{ GeV}/c^2$  [2]. The main obstacle in observing the single-top process is however not its small rate, but the large associated backgrounds. After all selection requirements are imposed, the signal to background ratio

---

\* Presented at the Symposium “Physics in Collision”, Annecy, France, June 26–29, 2007.

is close to  $1/15$ . This challenging, background-dominated dataset is the main motivation for using multivariate techniques in the CDF and  $D\bar{\theta}$  analyses presented here<sup>1</sup>.

## 2. CDF single-top searches

The CDF Collaboration has recently reported single-top results from analyzing the  $1 \text{ fb}^{-1}$  dataset. The event selection exploits the kinematic features of the signal final state, which contains a top quark, a bottom quark, and possibly additional light quark jets. To reduce multijet backgrounds, the  $W$  originating from the top quark is required to have decayed leptonically. This is achieved by demanding a high-energy electron or muon ( $E_T(e) > 20 \text{ GeV}$ , or  $P_T(\mu) > 20 \text{ GeV}/c$ ) and large missing energy from the undetected neutrino  $\cancel{E}_T > 25 \text{ GeV}$ . The backgrounds surviving these selections are  $t\bar{t}$ ,  $W$ +heavy flavor ( $Wb\bar{b}$ ,  $Wc\bar{c}$ ,  $Wc$ ), and diboson  $WW$ ,  $WZ$ , and  $ZZ$ . In addition, there is instrumental background from: “mis-tagged” events in which light flavor quarks are misidentified as heavy flavor jets, and “non- $W$ ” multijet events in which a jet is erroneously identified as a lepton. A large fraction of the  $t\bar{t}$  and the non-top backgrounds is further removed by demanding exactly two jets with  $E_T > 15 \text{ GeV}$  and  $|\eta| < 2.8$  be present in the event. At least one of the two tight jets should be tagged as a  $b$ -quark jet by using displaced vertex information from the silicon vertex detector.

TABLE I

Expected numbers of events, along with the observed event yields at CDF.

Process	$W + 2$ jets prediction
$t$ -channel	$22.4 \pm 3.6$
$s$ -channel	$15.4 \pm 2.2$
$t\bar{t}$	$58.4 \pm 13.5$
$Wb\bar{b}$	$170.9 \pm 50.7$
$Wc\bar{c}$	$63.5 \pm 19.9$
$Wc$	$68.6 \pm 19.0$
$W$ + light flavor (mis-tags)	$136.1 \pm 19.7$
$Z$ +jets	$11.9 \pm 4.4$
Diboson ( $WW, WZ, ZZ$ )	$13.7 \pm 1.9$
non- $W$	$26.2 \pm 15.9$
Total predicted	$587.1 \pm 96.6$
Observed	644

<sup>1</sup> The results presented here are current as of June 2007; for the latest results from the CDF and  $D\bar{\theta}$  Collaborations we point the reader to Ref. [3].

The expected and observed event yields corresponding to the  $1 \text{ fb}^{-1}$  dataset are given in Table I.

An Artificial Neural Network (ANN) was developed to increase the  $b$ -quark purity of the sample selected by the standard  $b$ -tagging algorithm. This extended ANN tagger exploits mainly the long lifetime of  $b$ -hadrons, the high  $b$ -quark mass, and the high decay multiplicity. Fig. 1 shows good shape agreement between the ANN output distributions for the  $W+2$  jet data and a sum of the individual background components normalized to data.

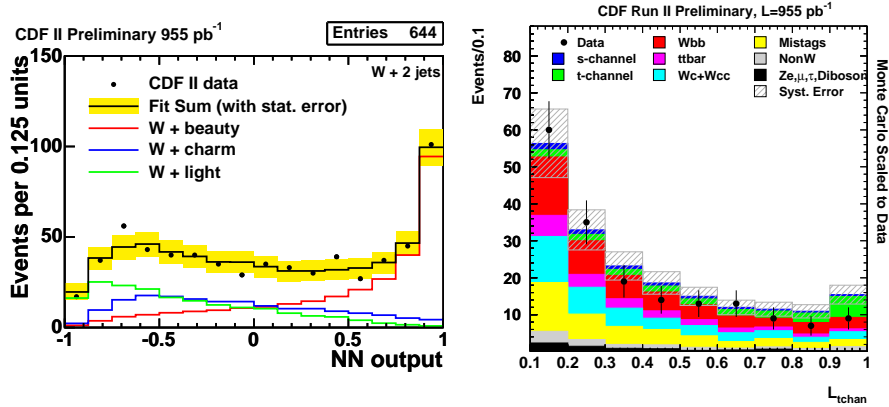


Fig. 1. Left: The ANN extended tagger output distributions for the CDF  $W+2$  jets events (points) compared to the Monte Carlo expectations. Right: Likelihood function discriminant  $\mathcal{L}_{t\text{-chan}}$  for the CDF data (points) compared to the expected distribution for  $1 \text{ fb}^{-1}$ .

### 2.1. CDF multivariate likelihood function analysis

In this analysis, the event variables  $(x_1, x_2, \dots, x_{n_{\text{var}}})$  are combined to construct the probability that a given candidate event originates from signal or background processes. The formula below is used to build likelihood function discriminants for  $s$ -channel and  $t$ -channel single-top:

$$\mathcal{L}(\{x_i\}) = \frac{\prod_{i=1}^{n_{\text{var}}} p_i^{\text{sig}}}{\prod_{i=1}^{n_{\text{var}}} p_i^{\text{sig}} + \prod_{i=1}^{n_{\text{var}}} p_i^{\text{bkg}}}, \quad p_i^{\text{sig}} = \frac{N_i^{\text{sig}}}{N_i^{\text{sig}} + N_i^{\text{bkg}}}. \quad (1)$$

The  $t$ -channel likelihood function is shown in Fig. 1. The data are more consistent with the background-only hypothesis, with a  $p$ -value [4] of 58.5% and the best fit for the  $s$ -channel and  $t$ -channel signal cross sections of  $\sigma_t = 0.2_{-0.2}^{+0.9} \text{ pb}$  and  $\sigma_s = 0.1_{-0.1}^{+0.7} \text{ pb}$ , respectively<sup>2</sup>.

<sup>2</sup> The Standard Model predictions are  $\sigma_t^{\text{SM}} = 2.0 \text{ pb}$ , and  $\sigma_s^{\text{SM}} = 0.9 \text{ pb}$ , respectively.

### 2.2. CDF artificial neural networks analysis

For this analysis three ANN's are developed, two of which are trained to identify the individual  $s$ -channel and the  $t$ -channel single-top processes, while the third one is trained to identify the combined  $s + t$  signal events. The three networks use the same input set of 23 event variables which are combined to form the three output discriminants  $\mathcal{O}_t$ ,  $\mathcal{O}_s$ , and  $\mathcal{O}_{s+t}$ . The left plot of Fig. 2 shows the signal region of the  $\mathcal{O}_{s+t}$  discriminant, in which a lack of candidate events is apparent. The fit to the data points yields a null result with a  $p$ -value of 54.6%, while the individual fits return:  $\sigma_t = 0.2^{+1.1}_{-0.2}$  pb and  $\sigma_s = 0.7^{+1.5}_{-0.7}$  pb, respectively.

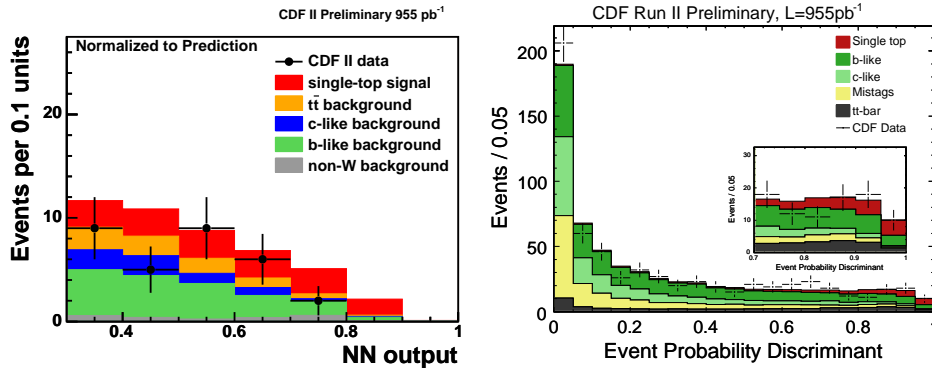


Fig. 2. Left: Data compared to Standard Model expectation in the signal region of the combined network output in the ANN search at CDF. Right: Event Probability Discriminant (EPD) distributions in the CDF matrix element analysis.

### 2.3. CDF matrix element analysis

In this technique, for every data and Monte Carlo event, the probabilities that the event originated from the signal or the different background processes are calculated [5]. The input to this analysis are the four-vectors of the measured jets and the charged lepton. The probability density results from the integration over the parton-level differential cross section which includes the matrix element from MadEvent [6], the parton distribution functions  $f(x_i)$ , and the detector resolutions parameterized by transfer functions  $W(x, y)$ . Assuming the lepton momenta and jet angles to be well-measured, the integration is performed over the quark energies and over the longitudinal component of the neutrino's momentum. With these probabilities in hand, we define:

$$\text{EPD} = \frac{b P_{\text{single-top}}}{b P_{\text{single-top}} + b P_{Wbb} + (1-b) P_{Wcc} + (1-b) P_{Wcj}}, \quad (2)$$

where  $b$  is the ANN extended tagger output mapped to the (0,1) interval. The EPD distribution is shown in Fig. 2, and the corresponding  $p$ -value is 1% ( $2.3\sigma$ ) providing a first hint of signal present in the CDF dataset. The best fit cross section is  $\sigma_{s+t} = 2.7_{-1.3}^{+1.5}$  pb.

A calculation of the compatibility among the three CDF analyses yields a compatibility level of 1%. Extensive checks have revealed no source responsible for this low value, other than statistical fluctuations. This will be verified with the larger dataset of  $2 \text{ fb}^{-1}$  already accumulated by CDF.

### 3. D $\emptyset$ single-top searches

The event selection at D $\emptyset$  resembles that of CDF presented in the previous section, but additionally includes the 3 and 4 jet channels. The expected and observed contributions are given in Table II.

TABLE II

Expected numbers of events, along with the observed event yields in the D $\emptyset$  single-top analyses.

Source	2 jets	3 jets	4 jets
$s$ -channel	$16 \pm 3$	$8 \pm 2$	$2 \pm 1$
$t$ -channel	$20 \pm 4$	$12 \pm 3$	$4 \pm 1$
$t\bar{t} \rightarrow \ell\ell$	$39 \pm 9$	$32 \pm 7$	$11 \pm 3$
$t\bar{t} \rightarrow \ell + \text{jets}$	$20 \pm 5$	$103 \pm 25$	$143 \pm 33$
$Wb\bar{b}$	$261 \pm 55$	$120 \pm 24$	$35 \pm 7$
$Wc\bar{c}$	$151 \pm 31$	$85 \pm 17$	$23 \pm 5$
$Wjj$ (light flavor)	$119 \pm 25$	$43 \pm 9$	$12 \pm 2$
Multijets (non- $W$ )	$95 \pm 19$	$77 \pm 15$	$29 \pm 6$
Total background	$686 \pm 41$	$460 \pm 39$	$253 \pm 38$
Data	697	455	246

#### 3.1. D $\emptyset$ boosted decision tree (DT) analysis

This analysis incorporates the information from 49 event variables. Of these, the ones providing the most discrimination power are the invariant mass of all jets  $M_{\text{jets}}$ , the invariant mass of the reconstructed  $W$  boson and the highest- $p_{\text{T}}$   $b$ -tagged jet  $M_{Wb_1}$ , the angle between the highest- $p_{\text{T}}$   $b$ -tagged jet and the charged lepton in the rest frame of the reconstructed top quark  $\cos\theta(\ell b_1)_{\text{jtop}}$ , and the lepton charge times the pseudorapidity of the untagged jet  $Q_\ell \times \eta_j$ . Both separate and combined  $s$ - and  $t$ -channel searches are performed in each of the 12 channels (two lepton types, three

jet bins, and two  $b$ -tag bins). Fig. 3 shows the high-discriminant region for the sum of all 12 combined search DT's. The measured cross section is  $\sigma_{s+t} = 4.9 \pm 1.4$  pb, and the corresponding significance is  $3.4\sigma$ , which establishes the first evidence for the single-top process. This result is also used to set limits on the value of  $|V_{tb}|$ :  $0.68 < |V_{tb}| \leq 1$  at 95% confidence level, assuming a pure  $V-A$  and CP conserving  $Wtb$  interaction, and that  $|V_{tb}|^2 \gg |V_{td}|^2 + |V_{ts}|^2$ . For a more in-depth discussion of this result we point the reader to the most recent  $D\emptyset$  publication [1].

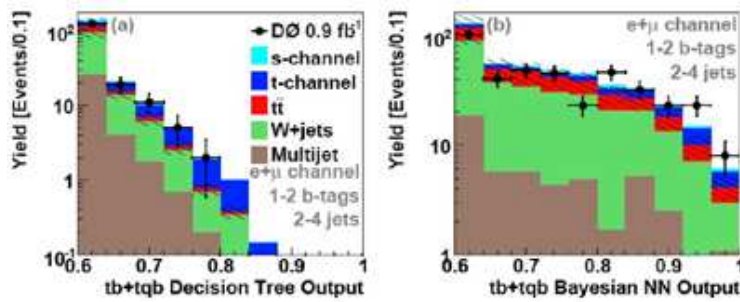


Fig. 3. Expected and observed output distributions for the  $D\emptyset$  DT analysis (left) and the BNN analysis (right).

### 3.2. $D\emptyset$ bayesian neural network (BNN) analysis

In the BNN analysis, a neural network is trained for each of the 12 search channels, with each network using between 18 and 25 input variables. The BNN output approximates the discriminant:

$$D(x) = \frac{f(x|S)}{f(x|S) + f(x|B)}, \quad (3)$$

where  $f(x|S)$  and  $f(x|B)$  are the probability densities for signal and background, and  $x$  denotes the variables that characterize the event. The observed BNN output distribution summed over the 12 channels is shown in Fig. 3. The observed  $p$ -value of 0.08% for this analysis corresponds to a  $3.1\sigma$  excess, while the measured cross section is  $\sigma_{s+t} = 4.4^{+1.6}_{-1.4}$  pb.

### 3.3. $D\emptyset$ matrix element analysis

The matrix element technique used in the  $D\emptyset$  single-top analysis uses the same general principles as described in the previous section, in addition including the  $W+3$  jets channel. The  $W+4$  jets channel is not included. For any event in these channels, a  $t$ -channel and a  $s$ -channel discriminant are calculated. The bidimensional space defined by these two discriminants

serves to extract the signal cross section of  $\sigma_{s+t} = 4.8_{-1.4}^{+1.6}$  pb, assuming the Standard Model cross section ratio  $\sigma_s/\sigma_t = 0.44$ . The  $p$ -value of 0.08% corresponds to a  $3.2\sigma$  excess.

In conclusion, all three  $D\theta$  analyses establish evidence for the single-top process. The results are combined using the Best Linear Unbiased Estimate (BLUE) method [7]. The correlations between pairs of analyses range between 59% (ME-BNN), and 66% (DT-BNN). The measured cross section is  $\sigma_{s+t} = 4.7 \pm 1.3$  pb with a significance of 3.6 standard deviations (Fig. 4).

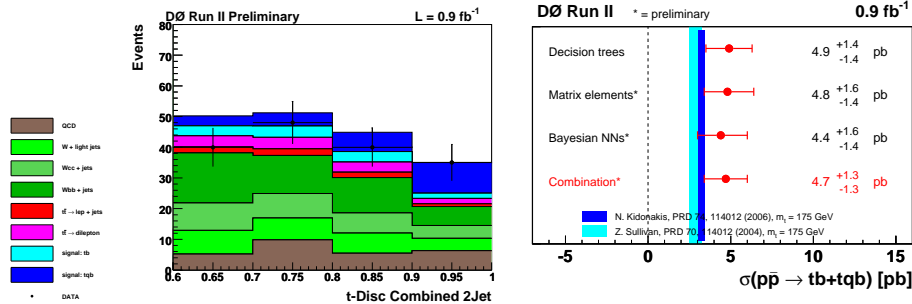


Fig. 4. Left: Expected and observed output distributions for the  $D\theta$  ME analysis. Right: Summary of the measured cross section results at  $D\theta$ , showing also the result from the BLUE combination technique.

#### 4. Beyond the standard model single-top production

In addition to the Standard Model analyses, the CDF and  $D\theta$  Collaborations have performed searches for single-top-quarks produced in exotic processes.

Recently, CDF has used the  $1 \text{ fb}^{-1}$  dataset to search for heavy  $W'$  bosons decaying to  $t\bar{b}$  pairs using the standard single-top event selection and analyzing the invariant mass spectrum of the reconstructed  $W'$  boson  $M(\ell\nu jj)$ . No significant evidence for a signal is observed and  $W'$  bosons with SM-like couplings to fermions [8] are excluded at the 95% confidence level (C.L.):  $M(W') > 760$  (790)  $\text{GeV}/c^2$  in case the right neutrino mass is smaller (larger) than  $M(W')$ . These results extend the  $W' \rightarrow t\bar{b}$  constraints previously set at the Tevatron [9].

The  $D\theta$  Collaboration has published [10] results from a  $230 \text{ pb}^{-1}$  search for anomalous production of single-top-quarks via flavor-changing neutral current couplings of a gluon to the top quark and a charm or an up quark. No significant deviation from the Standard Model predictions is observed, and upper limits at 95% C.L. are set on the anomalous coupling parameters  $\kappa_g^c/\Lambda$  and  $\kappa_g^u/\Lambda$ , where  $\Lambda$  is the scale of new physics and the  $\kappa$ 's are the strengths of the  $tcg$  and  $tug$  couplings:  $\kappa_g^c/\Lambda < 0.15 \text{ TeV}^{-1}$  and  $\kappa_g^u/\Lambda < 0.037 \text{ TeV}^{-1}$ .

## 5. Conclusions

We presented results from analyzing the  $0.9\text{--}1\text{ fb}^{-1}$  Tevatron datasets accumulated by the CDF and the  $D\bar{\theta}$  experiments. The expected sensitivities range from  $2.0\sigma\text{--}2.6\sigma$ , and  $1.9\sigma\text{--}2.2\sigma$  for the three CDF and the three  $D\bar{\theta}$  analyses, respectively. The CDF matrix element analysis measures a  $2.3\sigma$  signal excess over the background-only hypothesis, while the other two CDF analyses observe zero excess. All three  $D\bar{\theta}$  analyses establish evidence for single-top production, with the BLUE combination measuring a 3.6 standard deviations excess. The next goals of the Tevatron single-top program are the observation of the combined and individual single-top production channels, which will lead to greatly increased precision in the  $|V_{tb}|$  determination. The searches for exotic phenomena producing single-top-quarks are in a mature stage and will continue to play an important role in testing the Standard Model boundaries at the Tevatron.

We would like to thank our  $D\bar{\theta}$  and CDF colleagues who helped us to prepare this document. We also thank the organizers at LAPP who provided a very stimulating and enjoyable atmosphere during the conference.

## REFERENCES

- [1] D. Acosta *et al.* [CDF Collaboration], *Phys. Rev.* **D65**, 091102 (2002); *Phys. Rev.* **D69**, 052003 (2004); *Phys. Rev.* **D71**, 012005 (2005); B. Abbott *et al.* [ $D\bar{\theta}$  Collaboration], *Phys. Rev.* **D63**, 031101 (2001); V.M. Abazov *et al.* [ $D\bar{\theta}$  Collaboration], *Phys. Lett.* **B517**, 282 (2001); *Phys. Lett.* **B622**, 265 (2005); *Phys. Rev.* **D75**, 092007 (2006); *Phys. Rev. Lett.* **98**, 181802 (2007).
- [2] B.W. Harris *et al.*, *Phys. Rev.* **D66**, 054024 (2002); Z. Sullivan, *Phys. Rev.* **D70**, 114012 (2004); N. Kidonakis, *Phys. Rev.* **D74**, 114012 (2006).
- [3] [www-cdf.fnal.gov/physics/new/top/top.html](http://www-cdf.fnal.gov/physics/new/top/top.html) and [www-d0.fnal.gov/Run2Physics/top/top\\_public\\_web\\_pages/top\\_public.html](http://www-d0.fnal.gov/Run2Physics/top/top_public_web_pages/top_public.html)
- [4] A.L. Read, *J. Phys. G: Nucl. Part. Phys.* **28**, 2693 (2002).
- [5] V.M. Abazov *et al.* [ $D\bar{\theta}$  Collaboration], *Nature* **429**, 638 (2004); B. Stelzer, (Toronto Univ.) FERMILAB-THESIS-2005-79, UMI-NR07812 (2005).
- [6] F. Maltoni, T. Stelzer, *J. High Energy Phys.* **302**, 027 (2003).
- [7] L. Lyons, D. Gibaut, P. Clifford, *Nucl. Instrum. Methods* **A270**, 110 (1988).
- [8] Z. Sullivan, *Phys. Rev.* **D66**, 075011 (2002).
- [9] D. Acosta *et al.* [CDF Collaboration], *Phys. Rev. Lett.* **90** 081802 (2003); V.M. Abazov [ $D\bar{\theta}$  Collaboration], *Phys. Lett.* **B641**, 423 (2006).
- [10] V.M. Abazov *et al.* [ $D\bar{\theta}$  Collaboration], *Phys. Rev. Lett.* **99**, 191802 (2007).